EPJ Web of Conferences **113**, 04022 (2016)
DOI: 10.1051/epjconf/201611304022

Minimally non-local nucleon-nucleon potentials with chiral two-pion exchange including Δ's

Maria Piarulli[1,a]

[1]*Department of Physics, Old Dominion University, Norfolk, VA 23529, USA*

Abstract. A coordinate-space nucleon-nucleon potential is constructed in chiral effective field theory (χEFT) retaining pions, nucleons and Δ-isobars as explicit degrees of freedom. The calculation of the potential is carried out by including one- and two-pion-exchange contributions up to next-to-next-to-leading order (N2LO) and contact interactions up to next-to-next-to-next-to-leading order (N3LO). The low-energy constants multiplying these contact interactions are fitted to the 2013 Granada database in the laboratory-energy range 0–300 MeV.

1 Introduction

The recent history of nuclear physics has witnessed the tremendous development of nuclear chiral effective field theory (χEFT), originally proposed by Weinberg in a series of papers in the early 1990's [1]. The (approximate) chiral symmetry exhibited by the underlying theory of QCD in the low-energy regime severely restricts the form of the strong interactions among nucleons, Δ-isobars, and pions, as well as the electroweak interactions of these hadrons with external (electroweak) fields. In the specific case of two nucleons, the requirements imposed by χEFT can be incorporated into a non-relativistic quantum mechanical potential, constructed by a perturbative matching, order by order in the chiral expansion, between the on-shell scattering amplitude and the solution of the Schrödinger equation (see, for example, the review paper by Machleidt and Entem [2]). By its own nature, χEFT needs to be organized within a given power counting scheme and the resulting chiral potentials are conveniently organized in powers of Q/Λ_χ, where $Q \ll \Lambda_\chi$ is a general low-momentum scale entering the theory and $\Lambda_\chi \sim 1$ GeV specifies the chiral-symmetry breaking scale.

The objective of this presentation is to construct a coordinate-space chiral nucleon-nucleon (NN) potential derived up to next-to-next-to-next-to leading order (N3LO or Q^4) in the chiral expansion, including pions, nucleons and Δ-isobars degrees of freedom. The calculation of the potential is carried out by including one- and two-pion-exchange (OPE and TPE) contributions up to next-to-next-to-leading order (N2LO or Q^3) and contact interactions up to N3LO. While the OPE and TPE potentials represent the long-range part of the NN interaction, the contact terms, instead, encode the short-range physics, and their strength are specified by unknown low-energy constants (LEC's), which are then determined by fits to experimental data. The inclusion of Δ-isobars in the TPE component of the NN interaction is dictated from phenomenological considerations which explain the important role

[a]e-mail: mpiar001@odu.edu

of Δ isobars in nuclear structure and reactions [3]. The necessity to derive a coordinate-space chiral potential, whose natural formulation is in momentum-space, is related to the fact that many computational techniques utilized to calculate properties of nuclei and nuclear matter such as Quantum Monte Carlo (QMC) methods [4] require a local coordinate-space representation of the nuclear interactions. However, available momentum-space chiral potentials have the feature of being strongly non-local meaning that, upon Fourier transformation, they lead to non-local interactions (or **p**-dependent interactions, where $\mathbf{p} \longrightarrow -i\boldsymbol{\nabla}$ is the relative momentum operator) in coordinate-space. The sources of non-localities in χEFT are mostly due to contact interactions that depend not only on the momentum transfer $\mathbf{k} = \mathbf{p}' - \mathbf{p}$ but also on $\mathbf{K} = (\mathbf{p}' + \mathbf{p})/2$ ($\mathbf{p}$ and $\mathbf{p}'$ are the initial and final relative momenta of the two nucleons), and also to specific choices of cutoff functions. It is for this reason that we construct a chiral potential as local as possible by minimizing the number of non-localities due to contact interactions and removing those due to the choice of regulator functions. In order to make the short-range part as local as possible, we use Fierz identities to remove terms which in coordinate-space would lead to powers higher than two in the relative momentum operator **p**. However, while this chiral potential is local at N2LO [5, 6], terms proportional to p^2 still persist at N3LO [6]. To avoid non-localities due to regulators, we choose cutoff functions that depend only on the relative distance between the two nucleons.

2 Potentials

The *NN* potential presented in this work includes a strong interaction component derived from χEFT up to N3LO and denoted as v_{12}, and an electromagnetic interaction component, including up to terms quadratic in the fine structure constant α, and denoted as $v_{12}^{\rm EM}$. The $v_{12}^{\rm EM}$ component is the same as that adopted in the Argonne v_{18} (AV18) potential [7]. The component induced by the strong interaction is conveniently separated into long- and short-range parts, labeled, respectively, $v_{12}^{\rm L}$ and $v_{12}^{\rm S}$. The $v_{12}^{\rm L}$ part includes the OPE and TPE contributions up to N2LO, illustrated in Fig. 1: panel (a) represents the static OPE contribution at leading order (LO or Q^0); panels (b)–(g) represent the TPE contributions at next-to leading (NLO or Q^2) without and with Δ-isobars in the intermediate states; lastly, panels (h)–(m) represent sub-leading TPE contributions at N2LO. The open circles denote πN and $\pi N\Delta$ couplings from the sub-leading chiral Lagrangians $\mathcal{L}^{(2)}_{\pi N}$ [8] and $\mathcal{L}^{(2)}_{\pi N\Delta}$ [9]. The NLO and N2LO loop corrections contain ultraviolet divergencies, which are isolated in dimensional regularization and then reabsorbed into contact interactions by renormalization of the associated LEC's [10, 11]. Note that one-loop as well as two-loop TPE and three-pion exchange contributions at N3LO have been neglected, since their effect on the peripheral phase shifts would have negligible influence on the fit to the *NN* data (see, for example, Ref. [2] for a discussion on this issue). Furthermore it is the LEC's at Q^4 that are critical for a good reproduction of phase shifts in lower partial waves, particularly D-waves, and a good fit to the *NN* database in the 0–300 MeV range of energies considered in the present study. The LO and NLO terms depend on the the pion decay amplitude $F_\pi = 184.80\,\text{MeV}$, and the nucleon and N-to-Δ axial coupling constants, respectively $g_A = 1.29$ and $h_A = 3\,g_A/\sqrt{2}$. The sub-leading N2LO terms also depend on the LEC's c_1, c_2, c_3, and c_4 and the combination of LEC's $(b_3 + b_8)$, respectively from the second order πN and $\pi N\Delta$ chiral Lagrangians $\mathcal{L}^{(2)}_{\pi N}$ [8] and $\mathcal{L}^{(2)}_{\pi N\Delta}$ [9]. The values of these LEC's are determined by fits to πN scattering data and are given in [9]. Note that we retained the LEC $(b_3 + b_8)$ in our fit, even though it is redundant at this order [12].

The coordinate-space expressions for the TPE terms are obtained by using the spectral function representation [13], however with no spectral cutoff [14]. Therefore, the potential $v_{12}^{\rm L}$ reads [6]

$$v_{12}^{\rm L} = \left[\sum_{l=1}^{6} v_{\rm L}^{l}(r)\, O_{12}^{l}\right] + v_{\rm L}^{\sigma T}(r)\, O_{12}^{\sigma T} + v_{\rm L}^{tT}(r)\, O_{12}^{tT}\,, \tag{1}$$

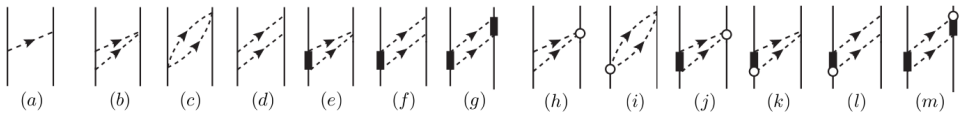

Figure 1. OPE and TPE contributions at LO [(a)], NLO [(b)–(g)], and N2LO [(h)–(m)]. Nucleons, Δ isobars, and pions are denoted, respectively, by the solid, thick-solid, and dashed lines; both direct and crossed box contributions are retained in diagrams (d), (f)–(g), (l)–(m). The open circles denote πN and $\pi N\Delta$ couplings from the sub-leading chiral Lagrangians $\mathcal{L}^{(2)}_{\pi N}$ [8] and $\mathcal{L}^{(2)}_{\pi N\Delta}$ [9].

with $O_{12}^{l=1,\ldots,6} = [\mathbf{1}\,,\,\boldsymbol{\sigma}_1\cdot\boldsymbol{\sigma}_2\,,\,S_{12}]\otimes[\mathbf{1}\,,\,\boldsymbol{\tau}_1\cdot\boldsymbol{\tau}_2]$ denoted as $c, \tau, \sigma, \sigma\tau, t, t\tau$, and $O_{12}^{\sigma T} = \boldsymbol{\sigma}_1\cdot\boldsymbol{\sigma}_2\,T_{12}$, and $O_{12}^{tT} = S_{12}\,T_{12}$, and $T_{12} = 3\,\tau_{1z}\tau_{2z} - \boldsymbol{\tau}_1\cdot\boldsymbol{\tau}_2$ is the isotensor operator. The terms proportional to T_{12} account for the charge-independence breaking induced by the difference between the neutral and charged pion masses in the only OPE. The radial functions $v_{\rm L}^{l}(r)$, $v_{\rm L}^{\sigma T}(r)$ and $v_{\rm L}^{tT}(r)$ are listed in [6]. They are singular at the origin (they behave as $1/r^n$ with n taking on values up to $n = 6$), and each is regularized by a cutoff of the form

$$C_{R_{\rm L}}(r) = 1 - \frac{1}{(r/R_{\rm L})^6\, e^{(r-R_{\rm L})/a_L} + 1}\,, \tag{2}$$

where three values for the radius R_L are considered $R_L = (0.8, 1.0, 1.2)$ fm with the diffuseness a_L fixed at $a_L = R_L/2$ in each case.

The potential $v_{12}^{\rm S}$ includes charge-independent (CI) contact interactions at LO, NLO and N3LO, and charge-dependent (CD) ones at LO and NLO, in momentum-space $v_{12}^{\rm S}(\mathbf{k},\mathbf{K}) = v_{12}^{\rm S,CI}(\mathbf{k},\mathbf{K}) + v_{12}^{\rm S,CD}(\mathbf{k},\mathbf{K})$, and their expressions are given in [6]. In the NLO and N3LO contact interactions terms proportional to K^2 and K^4, which would lead to p^2 and p^4 operators in coordinate space, have been removed by a Fierz rearrangement as discussed in Refs. [5, 6]. However, mixed terms of the type $k^2\,K^2$ or $\mathbf{K}\times\mathbf{k}$ cannot be Fierz-transformed away. In the potential $v_{12}^{\rm S,CD}(\mathbf{k},\mathbf{K})$ only terms up to NLO, involving charge-independence breaking (proportional to T_{12}) and charge-symmetry breaking (proportional to $\tau_{1z}+\tau_{2z}$), are accounted for. However, the LEC's associated with $\tau_{1z}+\tau_{2z}$, while providing some additional flexibility in the data fitting (especially the LO term which is necessary for reproducing the singlet nn scattering length), are not well constrained. The potential $v_{12}^{\rm S}$ in coordinate-space reads (see Ref. [6])

$$v_{12}^{\rm S} \;=\; \left[\sum_{l=1}^{19} v_{\rm S}^{l}(r)\,O_{12}^{l}\right] + \{\,v_{\rm S}^{p}(r) + v_{\rm S}^{p\sigma}(r)\,\boldsymbol{\sigma}_1\cdot\boldsymbol{\sigma}_2 + v_{\rm S}^{pt}(r)\,S_{12} + v_{\rm S}^{pt\tau}(r)\,S_{12}\,\boldsymbol{\tau}_1\cdot\boldsymbol{\tau}_2\;,\;\mathbf{p}^2\,\}\,, \tag{3}$$

where $O_{12}^{l=1,\ldots,6}$ have been defined above, $O_{12}^{l=7,\ldots,11} = \mathbf{L}\cdot\mathbf{S}\,,\,\mathbf{L}\cdot\mathbf{S}\,\boldsymbol{\tau}_1\cdot\boldsymbol{\tau}_2\,,\,(\mathbf{L}\cdot\mathbf{S})^2\,,\,\mathbf{L}^2\,,\,\mathbf{L}^2\,\boldsymbol{\sigma}_1\cdot\boldsymbol{\sigma}_2$, referred to as b, $b\tau$, bb, q, $q\sigma$, and $O_{12}^{l=12,\ldots,19} = [\mathbf{1}\,,\,\boldsymbol{\sigma}_1\cdot\boldsymbol{\sigma}_2\,,\,S_{12}\,,\,\mathbf{L}\cdot\mathbf{S}]\otimes\left[T_{12}\,,\,\tau_1^z+\tau_2^z\right]$ referred to as T, τz, σT, $\sigma\tau z$, tT, $t\tau z$, bT, $b\tau z$. The four additional terms, denoted as p, $p\sigma$, pt, and $pt\tau$, in the anti-commutator of Eq. (3) are $\mathbf{p}^2$-dependent. The radial functions $v_{\rm S}^{l}(r)$, $v_{\rm S}^{p}(r)$, $v_{\rm S}^{p\sigma}(r)$, $v_{\rm S}^{pt}(r)$ and $v_{\rm S}^{pt\tau}(r)$ are listed in [6]. The potential $v_{12}^{\rm S}$ is regularized via a Gaussian cutoff,

$$C_{R_{\rm S}}(r) = \frac{1}{\pi^{3/2}R_{\rm S}^3}e^{-(r/R_{\rm S})^2}\,, \tag{4}$$

and we consider, in combination with $R_L = (0.8, 1.0, 1.2)$ fm, $R_{\rm s} = (0.6, 0.7, 0.8)$ fm, corresponding to typical momentum-space cutoffs $\Lambda_{\rm S} = 2/R_{\rm S}$ from about 660 MeV down to 500 MeV.

3 Data analysis and results

The *NN* potential discussed in the previous section involves 34 unknown LEC's associated with the charge-independent contact interactions entering at LO, NLO and N3LO, and the charge-dependent contact interactions entering the LO and NLO. These contact parameters are determined by fitting the 2013 Granada database [15], consisting of 2309 *pp* and 2982 *np* data in the laboratory-energy range $E_{\rm lab} = 0 - 300$ MeV, as well as the deuteron binding energy. In the optimization procedure, as discussed in Ref. [6], we fit first phase shifts, then we refine the fit by minimizing the χ^2 obtained from a direct comparison with the database. In fact, sizable changes in the total χ^2 are found when passing from phase shifts to observables, so this refining is absolutely necessary to claim reasonable fits to data. This is a general feature which is often found, and reflects the different weights in the χ^2 contributions of the two different fitting schemes. Indeed, the initial guiding fit to phase shifts chooses a prescribed energy grid arbitrarily, which *does not* correspond directly to measured energies, nor necessarily samples faithfully the original information provided by the experimental data. Moreover, there are different PWA's which describe the same data but yield different phase shifts with significantly larger discrepancies than reflected by the inferred statistical uncertainties [15].

In Ref. [6] we report results for the potentials $v_{12} + v_{12}^{\rm EM}$ corresponding to three different choices of cutoffs $(R_{\rm L}, R_{\rm S})$: model a with (1.2, 0.8) fm, model b with (1.0, 0.7) fm, and model c with (0.8, 0.6) fm. The $\chi^2(pp)$/datum and $\chi^2(np)$/datum obtained by fitting the Granada database up to lab energies of 300 MeV are about 1.48, 1.48, 1.52 and 1.20, 1.19, 1.23 for models a, b, and c, respectively; the corresponding global $\chi^2(pp + np)$/datum are 1.33, 1.33, 1.37. Errors for *pp* data are significantly smaller than for *np*, thus explaining the consistently higher $\chi^2(pp)$/datum. The fitted values of the LEC's corresponding to models a, b, and c are listed in [6].

The S-wave, P-wave, and D-wave phase shits for *np* (in $T = 0$ and $T = 1$) and *pp* are reported in Ref. [6] where the calculated phases are compared to those obtained in partial-wave analyses (PWA's) by the Nijmegen [16], Granada [15], and Gross-Stadler [17] groups. There, we also provide tables of the *pp*, *np* and *nn* effective range parameters and of deuteron properties, including a figure of the deuteron S and D waves.

References

[1] S. Weinberg, Phys. Lett. **B251**, 288 (1990); Nucl. Phys. **B363**, 3 (1991); Phys. Lett. **B295**, 114 (1992).

[2] R. Machleidt and D.R. Entem, Phys. Rep. **503**, 1 (2011).

[3] R. Schiavilla *et al.*, Phys. Rev. C **45**, 2628 (1992).

[4] J. Carlson *et al.*, arXiv:1412.3081[nucl-th].

[5] A. Gezerlis *et al.*, Phys. Rev. Lett. **111**, 032501 (2013); Phys. Rev. C **90**, 054323 (2014).

[6] M. Piarulli *et al.*, Phys. Rev. C **91**, 024003 (2015).

[7] R. B. Wiringa, V. G. J. Stoks, and R. Schiavilla, Phys. Rev. C **51**, 38 (1995).

[8] N. Fettes *et al.*, Ann. Phys. **283**, 273 (2000).

[9] H. Krebs, E. Epelbaum, and Ulf.-G. Meißner, Eur. Phys. J. A **32**, 127 (2007).

[10] E. Epelbaum, W. Glöckle, and U.-G. Meissner, Nucl. Phys. **A637**, 107 (1998).

[11] S. Pastore *et al.*, Phys. Rev. C **80**, 034004 (2009).

[12] B. Long and V. Lensky, Phys. Rev. C **83**, 045206 (2011).

[13] E. Epelbaum, W. Glöckle, and U.-G. Meißner, Eur. Phys. J. A **19**, 125 (2004).

[14] N. Kaiser, R. Brockmann, and W. Weise, Nucl. Phys. A **625**, 758 (1997); Nucl. Phys. A **637**, 395 (1998).

[15] R. Navarro Pérez, J.E. Amaro, and E. Ruiz Arriola, Phys. Rev. C **88**, 064002 (2013); Phys. Rev. C **89**, 024004 (2014); Phys. Rev. C **89**, 064006 (2014).
[16] V.G.J. Stoks *et al.*, Phys. Rev. C **48**, 792 (1993); Phys. Rev. C **49**, 2950 (1994).
[17] F.L. Gross and A. Stadler, Phys. Rev. C **78**, 014005 (2008).